cAMP-Mediated Inhibition of Intracellular Particle Movement and Actin Reorganization in Dictyostelium

Deborah Wessels,* Noel A. Schroeder,* Edward Voss,* Anne L. Hall,‡ John Condeelis,‡ and David R. Soll*

* Department of Biology, University of Iowa, Iowa City, Iowa 52242; and ‡ Department of Anatomy and Structural Biology, Albert Einstein College of Medicine, Bronx, New York 10461

Abstract. Before addition of cAMP, *Dictyostelum* amoebae rapidly translocating in buffer are elongate, exhibit expansion zones primarily at the anterior end and filamentous actin (F-actin) localization primarily in the anterior pseudopodia. Intracellular particle movement is primarily in the anterior direction, and the average rate of particle movement is roughly five times the rate of cellular translocation. Within seconds after the addition of 10^{-6} M cAMP, there is a dramatic suppression of cellular translocation, an inhibition of pseudopod formation, a freeze in cellular morphology, a dramatic depression in intracellular particle movement, loss of F-actin localization in pseudopodia concomitant with relocalization of F-actin in the general cytoplasmic cortex under the plasma membrane, and a doubling of F-actin content. After 10 s, expansion zones are again visible at the cell perimeter, but they no longer are localized in the original anterior portion of the cell. There is a slight rebound in particle movement after 10 s, but particles with persistent tracks now show no directionality towards the original anterior portion of the cell, as they did before cAMP addition. Finally, in parallel with the resumption of peripheral expansion and the small rebound in particle movement, there is a decrease in total cellular F-actin to the untreated level. The pattern of microtubule organization is unaffected by the addition of cAMP.

During aggregation in the cellular slime mold *Dictyostelium discoideum*, cells in the center of an aggregation territory release the chemoattractant cAMP in a pulsatile fashion (3, 30, 40). Cells peripheral to the center respond by relaying the signal outwardly (6, 10) and by moving in a directed fashion towards the aggregation center (1). Because of the pulsatile nature of the original signal and the relay system, cAMP moves outwardly through the territory as a nondissipating wave. The extracellular cAMP signal is mediated by a cell surface receptor that is a member of the beta-adrenergic receptor family (15) and interacts with G proteins (16, 31).

To investigate the sequence of receptor-mediated biochemical events in the cAMP response, the standard protocol has been the rapid addition of cAMP to chemotactically responsive cells suspended in or perfused with buffer. Although the increase in cAMP in the cellular environment under these experimental conditions occurs at a far faster rate than during the front of a natural wave (35, 44), a number of rapid physiological responses have been demonstrated which probably play integral roles in cAMP-mediated chemotaxis. These changes include (*a*) the synthesis and release of cAMP (5); (*b*) the synthesis of cGMP (23); (*c*) myosin phosphorylation (19); (*d*) an influx of calcium ions (49); (*e*) proton release (18); (*f*) the methylation of proteins and phospholipids (22); and (*g*) actin polymerization (13) and association with the cytoskeleton (24).

Recently, the behavioral responses of cells to a rapid increase in cAMP were assessed. It was demonstrated that the rapid addition of cAMP to the peak concentration of the natural wave (10^{-6} M) results in an immediate decrease in velocity measured by centroid translocation (35, 43, 44, 46), an increase in directional change (44), an increase in roundness (13, 35, 44), and a decrease in net cytoplasmic flow measured by "differencing" (35).

Measurements have been made to correlate behavioral responses with changes in cytoskeletal organization during rapid increases in cAMP. The rapid addition of cAMP to 10^{-6} M results in two peaks of actin polymerization at ~10 and 60 s (13), two peaks of incorporation of filamentous actin (F-actin)[1] into the cytoskeleton at ~10 and 60 (7, 24), incorporation of the actin cross-linking protein ABP-120 into the cytoskeleton and pseudopods between 40–60 s (4, 7), and transient incorporation of myosin in the cytoskeleton at 25 s (7, 17). These observations have suggested a model in which the transition of cAMP-treated cells from elongate to round, referred to as the "cringe" (9), at 25 s is correlated with actomyosin-based contraction. In addition, subsequent pseudopod extension correlates with polymerization and cross-linking of actin in the cytoskeleton that may constitute part of the driving force for pseudopod extension (4, 7, 13).

However, these considerations do not account for the first rapid peak of actin polymerization (13) and incorporation of actin into the cytoskeleton (7, 24) by 10 s. In the present

study, we have assessed the immediate effects of cAMP (10^{-6} M) on cellular as well as intracellular motility (particle movement), actin and tubulin organization, F-actin content, and the shape of polar cells locomoting on a glass surface. It is demonstrated that within seconds after a polar, rapidly translocating cell experiences cAMP, there are dramatic decreases in cellular translocation, pseudopod extension, and intracellular particle movement, and a dramatic relocalization of F-actin, as well as an increase in actin polymerization. After 10 s of cAMP addition, the level of F-actin decreases and particle movement is reinitiated, but in this case, the original anterior directionality of particle movement is lost.

Materials and Methods

Growth and Development

Cells of strain AX3, clone RC3, were cloned and grown according to methods previously described (33). Development was initiated by washing cells free of nutrients and dispersing roughly 5.5×10^7 cells on a black filter (No. 29; Whatman Inc., Clifton, NJ) saturated with buffered salts solution (38) according to methods previously described (33). Under these conditions, the onset of aggregation (the "ripple stage") occurred at 7 h (32, 36).

Treatment with cAMP

Cells were washed from development pads at the onset of aggregation, washed twice with buffered salts solution, then resuspended as single cells in buffered salts solution at a final density of 3×10^4 cells/ml. Approximately 0.3 ml of cell suspension was inoculated into a Dvorak-Stotler chamber (Nicholson Precision Instruments, Inc., Gaithersburg, Maryland), the chamber closed, and the cells were allowed to settle for 5 min. This resulted in a cell density of 33/mm^2. The chamber was then placed on the stage of an inverted microscope (ICM 405; Carl Zeiss, Inc., Thornwood, NY) equipped with differential interference contrast optics (Nomarski optics), including a differential interference contrast-Ph condensor (NA = 1.4), 63× Planapo objective (NA = 1.4), and a lambda plate inserted into the analyzer.

The inlet tube of the chamber was connected to a reservoir containing buffered salts solution, and the outlet tube to a peristaltic pump. The flow rate of the pump was adjusted to 1.7 ml/minute resulting in replacement of chamber fluid every 7.7 s. The time required for the perfusion solution to travel from the reservoir through the inlet tube to the center of the chamber, where cells were monitored for behavior, was carefully measured with dye solutions. The time interval between the initial entrance of cAMP into the chamber center and the achievement of maximum concentration was measured by shifting to a solution containing dye, and measuring intensity with an Image-1 processor (Interactive Video Systems, Concord, MA). The time interval was estimated to be 8 s, and the accuracy of estimating zero time of the shift ± 1 s.

Measurements of Cell and Particle Movement

Cell behavior was recorded on three-quarter inch tape through a Newvicon video camera (C-2400-07; Hamamatsu Photonics K.K., Hamamatsu City, Japan). Tapes were analyzed for cell motility, morphometric changes, and differencing with the dynamic morphology system software package in the Expert Vision Integrated Analysis System (Motion Analysis Corp., Santa Rosa, CA) according to methods previously published (34, 37). In this system, the edge of the cell was digitally recorded as frequently as every frame, centroid position calculated, and instantaneous velocity determined using the central difference method (21). "Instantaneous velocity" for a cell in a given video frame (n) was calculated by drawing a vector from the centroid in the previous frame ($n - 1$) to the centroid in the subsequent frame ($n + 1$), and the length of the vector divided by $2\,\Delta t$, where Δt is the time interval between frames. "Difference pictures" were generated by superimposing the cell outline of a given frame on the cell outline of a previous frame (the interval in this study was 4 s).

Particle behavior was recorded on the same tapes used for analyzing cell behavior. Particle tracks were entered into the Expert Vision Integrated Analysis System employing a manual digitizer (SVUI, Iowa City, Iowa) with a program which compensates for distortion (SVUI). Particles were selected independently of size and tracked as long as they were in focus. Positions were recorded every 0.5 s. Instantaneous velocities of particles were calculated in the same manner described for translocation of the cell centroid.

Actin and Tubulin Staining

Cells were washed from development pads, washed twice with buffered salts solution, and a drop of cells, at a density of 4×10^5 cells/ml, placed on a 12-mm, ethanol-washed coverslip (280 cells/mm^2). Cells were allowed to adhere to the coverslip, reestablish their elongate shape, and resume rapid centroid translocation. After 5 min, the major portion of the buffered salts solution was suctioned from the coverslip, immediately replaced with 80λ of 10^{-6} M cAMP in buffered salts solution and incubated for either 6 or 15 s. As a control, 80λ of buffered salts solution lacking cAMP was applied to parallel preparations for 6 s. Because of the potential effects of aldehyde fixation on cell morphology and actin localization (12), two different methods were used to fix the cells for morphological analysis and actin staining. The first method included formaldehyde fixation (39). Solution was removed from the preparation coverslip at the end of the incubation period and the coverslip immediately flooded with 3.7% formaldehyde in PBS (137 mM NaCl, 2.4 mM KCl, 8.0 mM Na_2HPO_4, 1.5 mM KH_2PO_4, pH 7.3). After 10 min, the formaldehyde solution was removed and the coverslips washed 3 times with PBS. The remaining solution was aspirated from the coverslip and 80λ of 10 μM fluorescein-conjugated phalloidin in PBS pipetted over the coverslip. Cells were then incubated in the dark for 20 min, washed free of phalloidin with PBS, and the coverslip was inverted over a drop of mounting medium (100 μg/ml DABCO in gelvatol) on a microscope slide. Cells were photographed through an inverted microscope (ICM 405; Carl Zeiss, Inc.) equipped for fluorescence microscopy with a 100 W super pressure mercury lamp. These preparations were identical to those used to make biochemical measurements of F-actin content.

In the second procedure for actin staining, glutaraldehyde fixation was employed (13). Cells on coverslips were fixed by flooding with a solution containing 1% glutaraldehyde, 0.1% Triton X-100 in buffer solution (BS: 0.4 M KH_2PO_4. 0.4 M K_2HPO_4-$7H_2O$, 0.5 M Pipes, 0.1 M EGTA, 1.0 m $MgSO_4$, pH 6.8) for 5 min. Coverslips were then washed three times with BS containing 1 mg/ml $NaBH_4$. Coverslips were then treated with TBS (154 mM NaCl, 0.02% NaN_3, 20 mM Tris-HCl, pH 7.8) for 15 min, then stained in the dark for 45 min with TBS containing 10 μM fluorescein-conjugated phalloidin, 1% BSA, and 0.02% NaN_3. Coverslips were then rinsed 4 times in TBS containing 0.1% BSA, 0.02% saponin, and 0.02% NaN_3 and mounted in a drop of PBS containing 0.1 M *N*-propylgallate and 50% glycerol. In the experiments described here, the two fixation methods resulted in similar cell morphology and actin localization patterns.

For tubulin staining (48), cells on coverslips were fixed by flooding with 3.7% formaldehyde in PBS. Coverslips were then washed 4 times with PBS. Amoebae were postfixed by treatment with methanol for 9 min and permeabilized with acetone for 6 min at −10°C. Preparations were airdried, and then incubated for 1 h in a humidified chamber at 37°C with an antiserum to tubulin (YOL 1/34, a gift from J. Kilmartin, University Medical School, Cambridge, UK) diluted 1:100 in PBS, 1% BSA. Preparations were then washed 4 times with PBS and the second antibody (FITC-conjugated anti-rat IgG preabsorbed with fixed aggregating amoebae and diluted 1:25 in PBS, 1% BSA) added. Coverslips were incubated for 1 h at 37°C in a humidified chamber in the dark, rinsed 4 times with PBS, mounted in gelvatol containing 100 mg/ml DABCO, and photographed as above. Photographs were image processed with an Image-I processor (Interactive Video Systems, Inc.) using a sharpening convolution or differential edge enhancement.

Measurements of F-actin Content

Changes in the content of F-actin of cells on a glass surface in response to cAMP stimulation were measured by a modification of methods previously described (13). Cells were starved at a density of 9.2×10^7/37-mm filter for 7–8 h, rinsed from the filters with BS solution containing 3 mM caffeine (BS/caffeine), and settled at a final density of 800–1,000 cells/mm^2 onto 20 × 20-mm EtOH-cleaned glass coverslips placed in 35-mm Petri dishes. Caffeine treatment inhibits spontaneous cAMP signaling between cells and so reduces experimental noise. However, experiments in which caffeine was deleted from the buffer yielded similar results. Beginning 25 min after rinsing cells from filters, coverslips were flooded with BS/caffeine and aspi-

1. *Abbreviations used in this paper*: BS, buffer solution; F-actin, filamentous actin.

rated. A Pipetman (Rainin Instrument Co. Inc., Woburn, MA) was used to flood the coverslip from one corner with 0.5 ml stimulus solution (buffer with or without 10^{-6} M cAMP), then with 3.5 ml fix solution (20 mM KPO_4, 10 mM Pipes, 5 mM EGTA, 2 mM $MgCl_2$, pH 6.8, containing 3.7% formaldehyde (Sigma Chemical Co., St Louis, MO), and 0.1% Triton X-100). This method made it possible to obtain very early time points reproducibly. Cells were fixed for 20 min. The dishes were then aspirated and flooded with 3 ml saponin buffer (20 mM KPO_4, 10 mM Pipes, 5 mM EDTA, 2 mM $MgCl_2$, pH 6.8, containing 0.1% saponin). The coverslips were blotted, transferred to a parafilm surface (cell-side up), and stained with 0.1 ml of 0.5 μM rhodamine phalloidin (Molecular Probes, Inc., Junction City, OR) in saponin buffer for 45 min in a humidified, darkened chamber. Coverslips were rinsed in 3 ml saponin buffer, destained in MeOH (Baker Instruments Corp., Allentown, PA), and the amount of rhodamine phalloidin in the MeOH eluate was determined by comparison of fluorescence emission (excitation, 540 nm; emission, 575 nm) to standards of known concentration.

To control for changes in cell adhesiveness and retention on the coverslip during processing, the number of cells in five microscope fields (arranged diagonally across the coverslip) was counted after MeOH extraction. The number of cells on each coverslip was calculated, leading to the amount of rhodamine phalloidin per cell in each sample. The "relative F-actin content" in this case is the average amount of rhodamine phalloidin/cell in a cAMP-treated sample divided by the average amount of rhodamine phalloidin/cell in a buffer-treated sample.

Results

The Effect of 10^{-6} M cAMP on Cellular Velocity

Cellular velocity, calculated as the instantaneous velocity of centroid translocation (see Materials and Methods for calculation), was measured at 2 s intervals for 5 amoebae before and after a shift from 0 M to 10^{-6} M cAMP in a Dvorak-Stotler chamber (Fig. 1). Within 6 s after cAMP first entered the chamber, the mean instantaneous velocity decreased from roughly 0.40 μm/s to 0.08 μm/s, then rebounded slightly to 0.16 μm/s by 15 s. The low level of 0.08 μm/s represented changes in centroid position because of slight shape changes and did not represent persistent cellular translocation, as evidenced by reconstructed cellular paths. In the three representative paths of centroids in Fig. 1, *B*, *C*, and *D*, persistent translocation of the cell body rapidly ceased within seconds after entrance of cAMP into the chamber (noted by an arrow in each path).

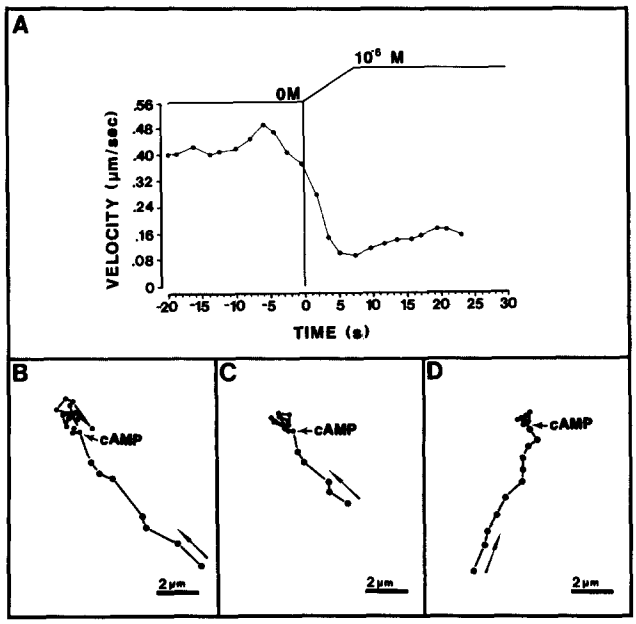

Figure 1. The effect of cAMP on cellular translocation. *A*, The mean instantaneous velocities of centroid translocation for five independently monitored cells are presented at time intervals before (−20–0 s) and after cAMP addition (0–30 s). *B*, *C*, and *D*, Examples of centroid tracks for three independent amoebae. Each dot represents the centroid position at 2 s time intervals. After cAMP addition, the dots are smaller to accommodate them in the area without changing scale. The estimated interval for the increase in cAMP concentration is diagramed at the top of *A*. Although there was virtually no real cell translocation after +2 s, mean instantaneous velocities of centroid translocation were measured as a result of shape change. This nonpersistent, random change in centroid translocation can be observed in the tracks in *B*, *C*, and *D* after cAMP addition. The arrows in *B*, *C*, and *D* represent direction of translocation.

The Effect of Stimulation with 10^{-6} M cAMP on Cell Shape

When amoebae were allowed to settle on the glass chamber

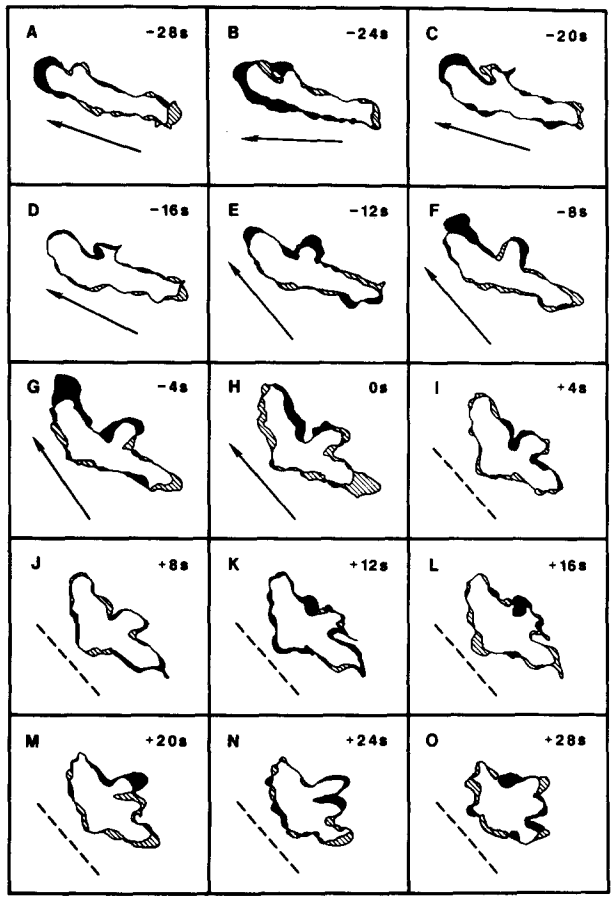

Figure 2. Difference pictures of amoebae before and after the addition of cAMP. The image in each panel represents the cell image at the time presented in the upper right hand corner superimposed on the cell image 4 s earlier. Expansion zones are filled, the contraction zones are hatched, and the common zones are unfilled. Zero time (0 s) indicates the estimated time, ±1 s, at which cAMP was added. It is obvious from the loss of the expansion zone in *H* (0 s) that cAMP had already entered the cellular environment at 0 s in this particular experiment. The direction of centroid translocation is presented in *A–H* (−28–0 s) as an arrow. This axis is presented in the figures after cAMP addition (+4–28 s) as a dashed line. Note the posterior contraction in *H (0 s)* followed by a relative freeze in cellular morphology in *I–K* (4–12 s).

wall and were perfused with buffered salts solution lacking cAMP, they moved in a highly polar fashion (35, 43). Most pseudopodial expansion occurred in the anterior half to third of the cell. In Fig. 2, *A–G*, "difference pictures" (see Materials and Methods) as well as the direction of translocation (*arrows*) are presented every 4 s for a representative amoeba perfused with buffered salts solution lacking cAMP. It is clear that expansion zones predominated in the anterior portions and contraction zones in the posterior portions of the cell. Immediately after cAMP first entered the chamber (*OS*), anterior expansion zones were dramatically reduced in all 15 cells examined in this fashion. In five of the cells, exemplified by the cell in Fig. 2, this reduction was accompanied by an immediate contraction of the posterior portion of the cells (Fig. 2 *H*). In the remaining 10 cells, extensive contraction was not observed. All cells appeared paralyzed for roughly the first 10 s after cAMP entered the chamber. After roughly 12 s in all of the 15 cells monitored, expansion zones were again evident, but no longer limited to the anterior portion of the cell (Fig. 2, *K–O*). By 24 s, cells had lost their original elongate shape in the axis of centroid translocation (compare cell shapes to original axis, presented as a dashed line in Fig. 2, *I–O*). Therefore, the most striking aspects of cAMP addition were (*a*) the relative freeze in shape accompanying the cessation of cellular translocation during the first 10 s; (*b*) nonaxial expansion after 10 s; and (*c*) the subsequent loss of cellular polarity.

The Effects of Stimulation with 10^{-6} M cAMP on Particle Movement

To assess the effects of cAMP on intracellular motility, video recordings of intracellular particles were analyzed by manually digitizing particle tracks into the computer assisted dynamic morphology system (see Materials and Methods). Particles were visualized with differential interference contrast (Nomarski) optics, and examples of the types of particles that were monitored are noted by arrows in three separate cells in Fig. 3, *A–C*. Particles ranged in size from 0.2 to 0.7 μm and presumably represent membrane bound vesicles (29). Particles moved in and out of the plane of focus and in some cases crossed paths. Therefore, some particles were monitored for extended periods before and after the shift, while others were monitored for as short a period as 5 s. Particles were selected randomly, without regard to size or position in the cell. Instantaneous velocity (see Materials and Methods) was calculated for each particle every 0.5 s. In Fig. 4, instantaneous particle velocities (each dot represents the instantaneous velocity of a single particle at a particular time point) are plotted throughout a shift experiment for each of five cells (Fig. 4, *A–E*), and the combined data for the five cells are coplotted in Fig. 4 *F*. Before the addition of cAMP, particles moved at velocities ranging between 0.0 and 3.5 μm/s with an average instantaneous velocity of 1.4 μm/s (calculated from the combined data in Fig. 4 *F* during the period preceding cAMP addition). Very few particles were immobile (i.e., exhibited an instantaneous velocity of 0.0). Within 2 s after cAMP first entered the chamber, the average instantaneous particle velocity decreased (Fig. 4, *A–F*). Between 1 and 10 s after initial entrance of cAMP into the chamber, few particles moved with instantaneous velocities above 1.0 μm/s, and a dramatic increase occurred in the

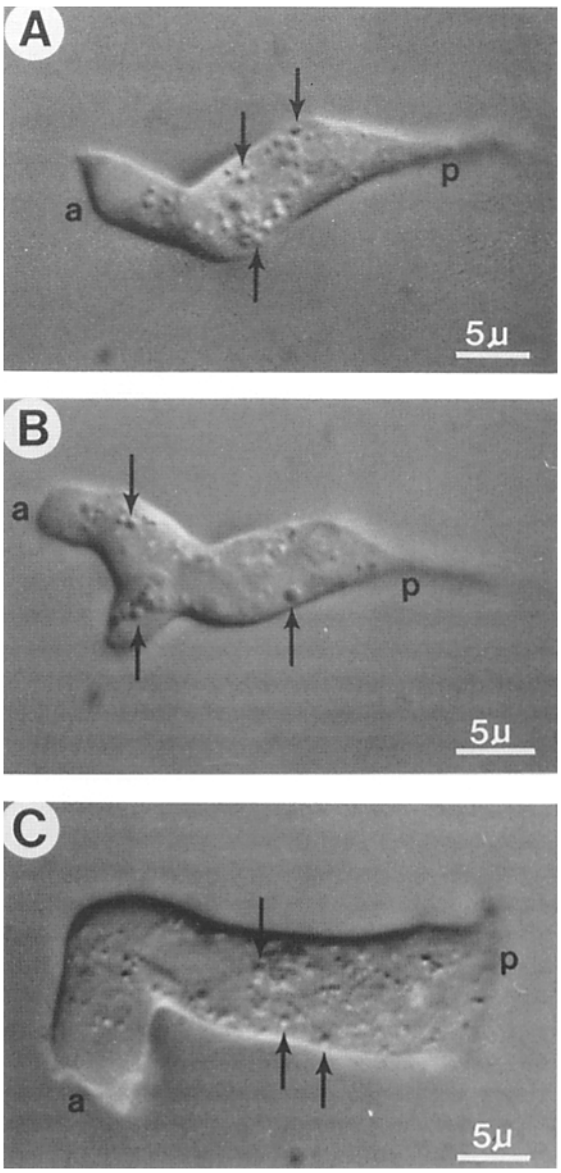

Figure 3. Examples of the types of intracellular particles monitored in three rapidly translocating cells. Arrows point to particles. *a*, anterior; *p*, posterior.

number of particles measured with instantaneous velocities of 0.0 μm/s (Fig. 4, *A–F*). The average instantaneous velocity during this 10-s period was 0.46 μm/s, roughly one-third the average particle velocity before cAMP addition.

A partial rebound in instantaneous particle velocities occurred between 8 and 20 s after cAMP first entered the chamber of the cells in Fig. 4, *A*, *B*, *D*, and *E*. This rebound began at roughly the time cAMP had reached the final shift concentration of 10^{-6} M in the chamber and was most obvious in the plot of composite data in Fig. 4 *F*. However, it should be noted that the majority of particles after 10 s still exhibited depressed velocities, and the proportion of immobile particles remained high.

The direction as well as the speed of particle movement was affected by the addition of cAMP. In Fig. 5 *A*, difference pictures are presented for four representative cells immedi-

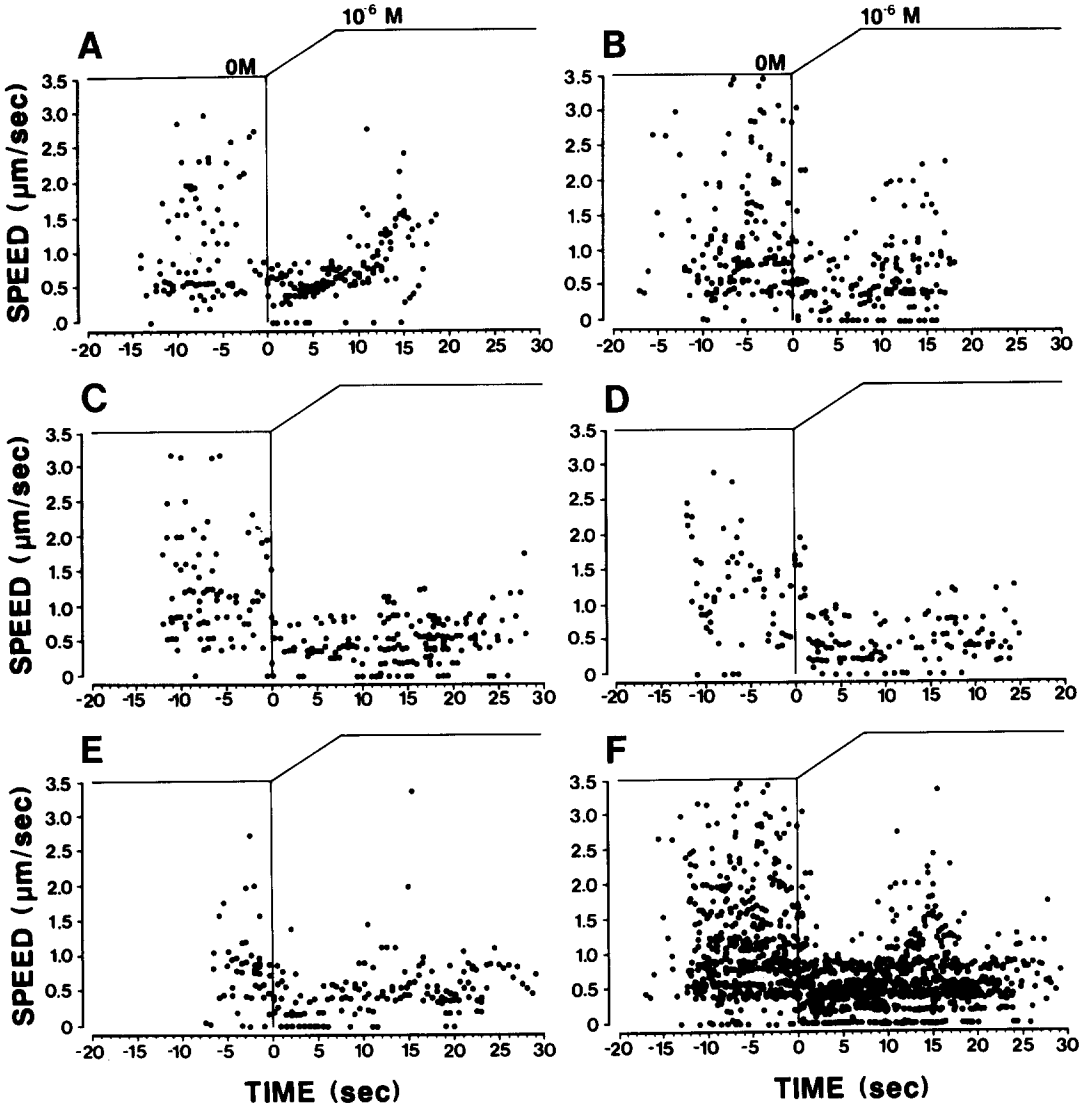

Figure 4. Particle velocity before and after the addition of 10^{-6} M cAMP. *A–E* represent measurements of the instantaneous velocities of particles for five individual cells. *F* is a composite plot of the instantaneous velocities of particles in the five cells in *A–E*. At least 15 particles were monitored for various lengths of time before and after cAMP addition for each cell. The estimated dynamics of the increase in cAMP concentration are presented above each plot and a vertical line indicating the estimated time (± 1 s) that cAMP entered the perfusion chamber (see Materials and Methods) is drawn through each plot.

ately before the addition of cAMP. Tracks of rapidly moving representative particles generated from particle position every 0.5 s are presented for each cell before cAMP addition (pre-cAMP), during the 10-s period after initial entrance of cAMP into the chamber (cAMP:0–10 s), and during the next 10-s period (cAMP:10–20 s). It should be noted that the scale for particle tracks in the particle movement panels is roughly half that for the difference pictures. Before cAMP addition, most particles moved in the axis of centroid translocation (compare the direction of particle tracks with the direction of centroid translocation indicated by arrows in the lower left-hand corner of each panel), even when particle movement was retrograde (Fig. 5, *A* and *C*; pre-cAMP particle movement). The averaged velocities of anterior moving particles in cells *A*, *B*, *C*, and *D* ranged between 1.4 and 2.9 μm/s. The velocities of centroid translocation of cells *A*, *B*, *C*, and *D* were 0.45, 0.50, 0.44, and 0.32 μm/s, respectively, during the same periods. The percent of particle velocities attributable to the forward movement of the cells ranged between 13 and 28%, and averaged 20% (±SD 5%). Therefore, the forward progress of these particles was on average roughly five times the velocity of anterior cellular translocation, and the major portion could therefore not be attributed to cellular translocation.

Between 0 and 10 s after the initial entrance of cAMP into the chamber, particles (Fig. 5, *A–D*; cAMP:0–10 s) exhibited nonaxial, depressed movement reminiscent of brownian motion. No directionality could be inferred from the particle plots. Between 10 and 20 s, the subset of particles exhibiting a rebound in velocity once again exhibited persistent paths, but did not follow the original axes of the cells (compare the direction of particle tracks with the direction of centroid translocation before cAMP addition noted by the arrow in the lower left corner of each panel under cAMP:10–20 s in Fig.

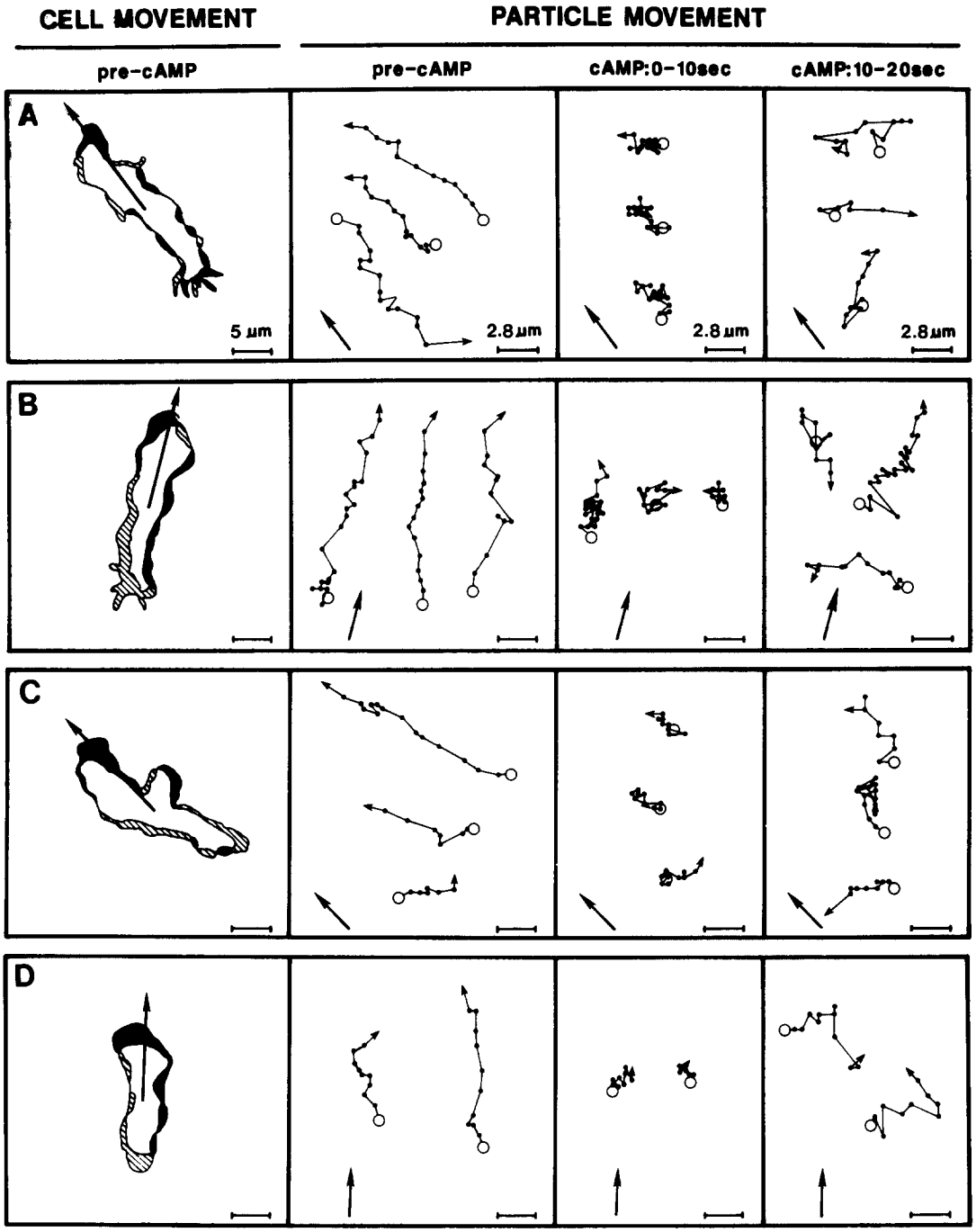

Figure 5. The direction of particle movement in relation to the cellular axis before and after addition of 10^{-6} M cAMP. A difference picture is presented in the first panel of *A–D* for four individual cells before cAMP addition. Representative tracks of particles in each cell are presented before cAMP addition (*pre-cAMP*), between 0 and 10 s after cAMP first entered the perfusion chamber (cAMP:0–10 s), and between 10 and 20 s after cAMP entered the chamber (cAMP:10–20 s). The arrows in the lower left-hand corners of each panel represent the direction of centroid translocation before cAMP addition. In each particle track, the unfilled circle represents the origin of the particle, or position at time zero. The arrow head at the end of the track represents the position of the particle at the last time point. The position of the particle was measured every 0.5 s. Tracks were drawn of rapidly moving particles without regard to particle size or cytoplasmic location. Note the scale for the cells in the left-hand panels is roughly twice the scale for the panels containing particle tracks.

5). The directions of rebounding particles appeared to be random.

The Effects of cAMP on F-actin Organization and Content

Within a few seconds after cAMP first entered the perfusion chamber, cells exhibited a decrease in the velocity of centroid translocation, a depression in anterior expansion zones, a temporary freeze in cell shape, and a depression in particle movement. These changes suggested that a reorganization of the cytoskeleton occurred immediately after the addition of cAMP.

To test the effects of cAMP on F-actin distribution, cells were stained with fluorescein-labeled phalloidin after either formaldehyde or glutaraldehyde fixation (see Materials and Methods). In the control cell populations (no cAMP addition), 90% or more of the cell population exhibited the elongate morphologies characteristic of rapidly translocating cells (Table I, *A*, *a*). The majority of these cells exhibited intense phalloidin staining in anterior pseudopodia (Table I, *A*, *b*: Fig. 6, *A–C*). Therefore, before cAMP treatment, rapidly translocating cells contained high concentrations of F-actin primarily in anterior pseudopodia.

In cell populations treated with 10^{-6} M cAMP for 6 s, 85% or more of the cell population still exhibited relatively elongate morphologies (Table I, *B*, *a*). However, only 15% or less of these cells exhibited intense phalloidin staining in anterior pseudopodia (Table I, *B*, *b*), and even in these few cases the staining was far less intense than stained pseudopodia in control cells. This represents a fivefold or more decrease in the proportion of elongate cells exhibiting intensely staining pseudopodia after 6 s of cAMP treatment. The proportion of elongate cells without intense F-actin staining in pseudopodia (Fig. 6, *D–F*) increased to 85% or more (Table I, *B*, *b*). These cells did exhibit an increase in staining in the cortical region just below the plasma membrane (Fig. 6, *D–F*).

It had previously been demonstrated that the whole cell content of F-actin increases for cells in suspension after stimulation with cAMP for 6 s (13). Thus, either cells in suspension respond differently to cAMP treatment when compared to cells on a surface, or the net amount of F-actin in cells on a surface is also greater after stimulation with cAMP, possibly because of global polymerization of actin despite localized loss of staining intensity in the anterior pseudopodia. To resolve this question, the whole cell content of F-actin in cells stimulated with cAMP while moving on a glass coverslip was measured. The method was designed to compensate for loss of cells because of changes in cell adhesiveness or retention on the coverslip during the experiment. The resulting measurement, relative F-actin content, reflects the changes in average F-actin content per cell in a cAMP-stimulated sample when compared to an untreated control sample (see Materials and Methods).

An increase in the relative F-actin content was detected as early as 2 s after cAMP addition (Fig. 7). F-actin content almost doubled between 2 and 6 s and returned to prestimulus levels by 20 s after cAMP addition (Fig. 7). Together these results demonstrate that the immediate response of elongate, motile cells to cAMP includes both a rapid increase in F-actin content and a rapid relocalization of F-actin involving loss of dense F-actin regions within pseudopodia and an increase in F-actin in the cytoplasmic cortex.

In cell populations treated with 10^{-6} M cAMP for 15 s, the proportion of elongate cells in the cell population dropped to 69% or less, and only 8% or less of these cells exhibited intense phalloidin staining in anterior pseudopodia (Table I, *C*, *b*). Again, these pseudopodia were not as intensely stained as untreated control cells, and just as in the 6-s treated cells, there was an increase in cortical staining just under the plasma membrane. It should be noted that at 15 s, cells had begun to lose polarity, and small expansion zones appeared in an apolar fashion (Fig. 2). This form of cellular expansion did not appear to be accompanied by the kind of intense F-actin localization that is associated with apical pseudopodial extension in actively translocating cells.

Table I. The Proportion of Elongate Cells with Dense F-actin Localization in Pseudopodia

	(*a*) Proportion of cell population with elongate morphology (%)	(*b*) Proportion of elongate cells with actin-filled pseudopodia (%)	(*c*) Number of cells scored
(*A*) Control (−cAMP) formaldehyde-fixed	94.4	65.0	176
Control (−cAMP) glutaraldehyde-fixed	90.2	81.0	93
(*B*) 10^{-6} M cAMP (6 s) formaldehyde-fixed	93.6	6.7*	111
10^{-6} M cAMP (6 s) glutaraldehyde-fixed	85.0	14.8*	87
(*C*) 10^{-6} M cAMP (15 s) formaldehyde-fixed	64.7	4.4*	176
10^{-6} M cAMP (15 s) glutaraldehyde-fixed	69.4	8.4*	206

Control cells were incubated on coverslips in buffer lacking cAMP for 5 min, then treated with buffer lacking cAMP for an additional 6 s before fixation. Test cells were incubated on coverslips in buffer lacking cAMP for 5 min, then treated with buffer containing 10^{-6} M cAMP for 6 or 15 s before fixation. Cells were fixed (see Materials and Methods for details) with either formaldehyde in phosphate buffer (formaldehyde-fixed) or glutaraldehyde in low ionic strength buffer (glutaraldehyde-fixed). Cells were scored as elongate when their length was 2–4× their diameter (see shapes in Fig. 2 *A–G*). Nonelongate cells exhibited no obvious cell polarity (see shape in Fig. 2 *N* and *O*).
* Pseudopod staining in these cases was far less intense than in the controls in *A* and *B*.

The Effects of cAMP on Tubulin Organization

Since microtubules have been implicated in particle movement (8, 26), and the addition of cAMP immediately depresses particle movement, we examined whether the addition of cAMP had an immediate effect on microtubule organization. The organization of microtubules in elongate cells rapidly translocating on a glass surface in buffer and 6 s after addition of cAMP were compared. In 82% of untreated elongate cells (Table II, *A*, *b*), microtubules emanated from a single microtubule organizer center with predominantly anterior–posterior orientation (Fig. 8, *A–C*). In 18% of untreated elongate cells (Table II), microtubules exhibited a randomly dispersed pattern. 6 s after the addition of cAMP, the population of cells exhibited roughly the same proportion of elongate cells and roughly the same proportion of elongate cells with microtubules exhibiting anterior–posterior orientation (Table II, *B*, *b*, Fig. 8, *D–F*). The population of elongate cells with axially oriented microtubules were further categorized into those with predominantly anteriorly oriented microtubules and those with microtubules equivalently oriented anteriorly and posteriorly. Again, there was no

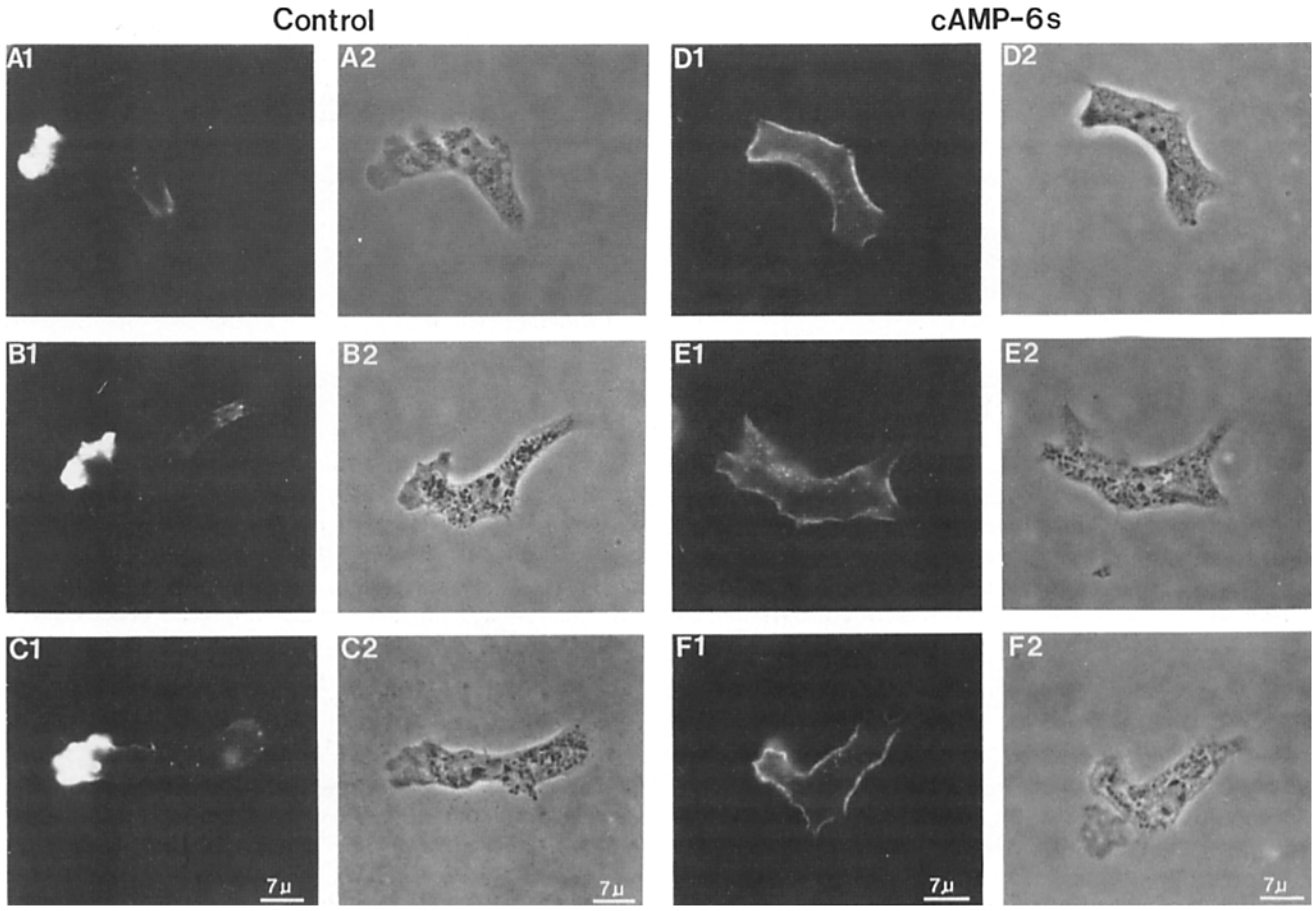

Figure 6. F-actin localization in untreated, rapidly translocating control cells (*A–C*) and in cells treated with cAMP for 6 s (*D–F*). Cells were fixed with glutaraldehyde and stained with fluorescein-conjugated phalloidin according to the procedure described in Materials and Methods. The fluorescent micrograph of each cell is present in *1* and the corresponding phase-contrast micrograph in *2*.

significant difference between control and cAMP-treated cells (data not shown). Therefore, in contrast to the rapid effects of cAMP on actin organization and polymerization, there was no comparable effect on microtubule organization.

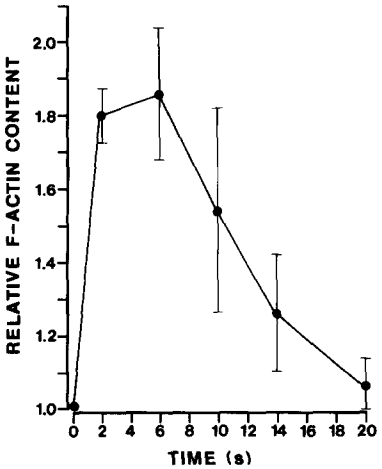

Figure 7. Changes in F-actin content of cells in response to the addition of 10^{-6} M cAMP. Relative F-actin content is the ratio of the amount of rhodamine-labeled phalloidin staining in a cAMP-stimulated sample to the amount of staining in a buffer-treated sample (see Materials and Methods). $n = 4 - 7$ and error bars show standard deviation of the mean (except at 10 s, where $n = 2$ and error bars represent the range).

Discussion

Aggregation competent amoebae of *Dictyostelium* move on glass in the absence of cAMP at average speeds of 0.4 μm/s and exhibit an elongate morphology. They are highly polarized with new pseudopodial extensions densely filled with F-actin forming predominantly in the anterior portion of the cell. The rapid addition of 10^{-6} M cAMP has an immediate effect on their motility. Within seconds after addition, the velocity of centroid translocation and anterior pseudopod formation decrease dramatically. After roughly 10 s, expansion zones discriminated by differencing of the cell periphery begin to appear, but they are smaller than the anterior pseudopodia of rapidly translocating amoebae, and they appear randomly around the cell's circumference, resulting in the loss of the elongate shape of the cell after 20 s, a process that most probably represents the "cringing" response noted in previous studies of shape changes following the rapid addition of cAMP to aggregation-competent amoebae (9, 13, 43).

Amoebae moving on glass in the absence of cAMP also exhibit polarized intracellular particle movement. Most particles move in a persistent fashion in the same direction as cellular translocation at velocities that average 1.4 μm/s, but which are as high as 3.5 μm/s. The velocities of particles moving in the anterior direction in a rapidly translocating cell are on average five times the velocity of cellular translocation. Since these particles do not accumulate in the an-

Table II. Proportions of Cells Exhibiting Different Morphologies and Tubulin Staining Patterns

	(*a*) Proportion of cell population with elongate morphology (%)	(*b*) Proportion of elongate cells with predominantly axial microtubules (%)	(*c*) Proportion of elongate cells with randomly dispersed microtubules (%)	(*d*) No. of cells scored
(*A*) Control (−cAMP)	95	82	18	96
(*B*) 10 M cAMP (6 s)	92	80	20	105

Control cells were incubated on coverslips in buffer lacking cAMP for 5 min, then treated with buffer lacking cAMP for an additional 6 s before fixation. Test cells were incubated on coverslips in buffer lacking cAMP for 5 min, and then treated with buffer containing 10^{-6} M cAMP for 6 s before fixation. Cells were scored as elongate when their length was 2 to 4× their diameter, and nonelongate when they exhibited no obvious polarity.

terior portion of the cell, they must either recycle to the rear, which has not been observed, or lose their integrity when they reach the particulate cytoplasm–pseudopod interphase. Roos et al. (29) measured particle movement in undifferentiated amoebae of *Dictyostelium discoideum*, and recorded average measurements of 2.8 μm/s for small particles, 2.1 μm/s for large particles and 2.1 μm/s for very large particles. They did not observe polar particle movement, but micrographs of their cells indicated that they lacked axial polarity (i.e., they were not elongate) (29), and, since they employed vegetative cells grown in the absence of bacteria, the cells were most likely not translocating in a rapid and persistent fashion (45).

The rapid addition of 10^{-6} M cAMP to a rapidly moving amoeba results in an almost immediate depression in the rate of particle movement. Particles with increased velocity are again observed 10 s after cAMP addition, but they do not exhibit the axial orientation exhibited by the majority of rapidly moving particles before cAMP addition. This loss of axial orientation coincides with the random orientation of new expansion zones and the incapacity of the cell body to translocate in a persistent fashion.

The relationship of particle movement and the cytoskeleton has long been a focus of investigation (e.g., 2, 11, 28, 29). Therefore, we tested whether parallel cytoskeletal events accompanied the depression in particle movement and cellular motility immediately after cAMP addition. The most surprising result was the rapid decrease of F-actin in pseudopodia, and the concomitant increase in F-actin in the cortical shell, just under the plasma membrane. This rapid reorganization is accompanied by a transient increase in total cell F-actin measured by a phalloidin-binding assay (13). It seems likely that the rapid loss of pseudopodial F-actin is related to the immediate cessation of centroid translocation, but it is not clear if the rapid increase or relocalization of actin is

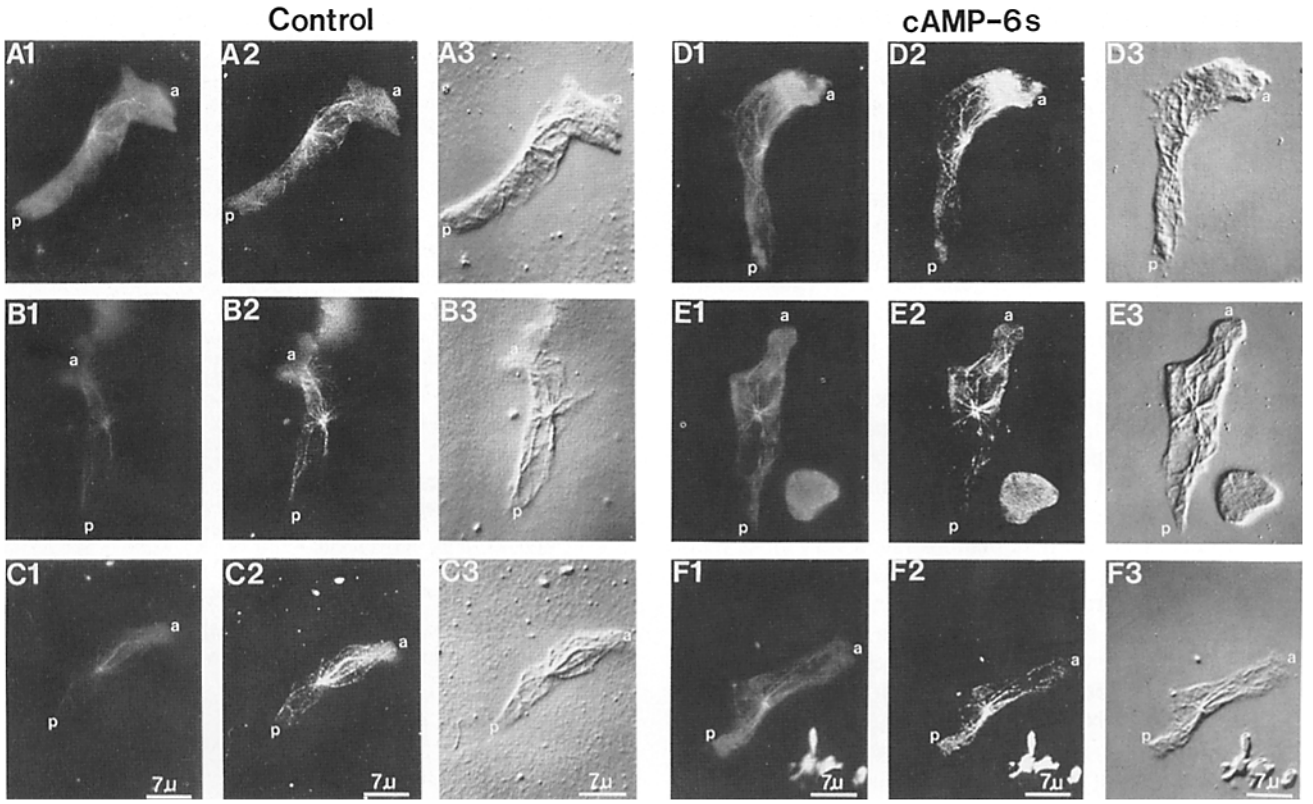

Figure 8. Microtubule distributions in untreated controls cells (*A–C*) and in test cells treated with 10^{-6} M cAMP for 6 s (*D–F*). *A1*, *B1*, *C1*, fluorescent micrographs of three control cells stained with an antiserum to tubulin (see Materials and Methods); *D1*, *E1*, *F1*, and fluorescent micrographs of three test cells stained with antiserum to tubulin. In *A2–F2*, the micrographs of the cells in *A–F* were enhanced by image processing using a sharpening convolution. In *A3–F3*, the micrographs of the cells in *A–F* were enhanced by image processing using differential edge-enhancement to generate a pseudo-three-dimensional image.

related to the cessation of particle movement. Several lines of evidence suggest that microfilaments are involved in intracellular particle movement (e.g., 2, 11, 14), and the immediate increase in total F-actin content by 80% within 2 s of cAMP addition suggests that F-actin gelation may be responsible for the concomitant depression in cellular translocation and intracellular particle movement. Because microtubules have long been implicated in intracellular particle movement and because it was previously demonstrated that the microtubule inhibitor nocodazole reduces saltatory particle movement over a 3-h period in growing *Dictyostelium* amoebae (29), the immediate effect of cAMP on microtubule organization was also examined. As far as could be told from static immunostained preparations, the general organization of the microtubule organizing center and the orientation of microtubules in relation to cell polarity were retained after cAMP addition. However, this in no way implies that the dynamic characteristics of cytoplasmic microtubules and associated proteins are unaffected by cAMP.

The time course for the stimulation of actin polymerization by the addition of 10^{-6} M cAMP reported here correlates reasonably closely with the rapid rise (1–3 s) and peak (3–7 s) of F-actin association with the cytoskeleton, as reported elsewhere (7, 24). However, the fact that this increase appears to represent cortical and not pseudopodial F-actin, as has been assumed (e.g., references 17, 27), may explain why this early peak is biochemically and kinetically distinct from subsequent ones (13, 25), which we have demonstrated are most likely pseudopodial (13). In addition, it should be noted that the inhibition and recovery of intracellular particle motility, and the dynamics of F-actin levels and F-actin relocalization induced by 10^{-6} M cAMP correlate with the time course of stimulated cGMP levels as reported by Van Haastert and associates (41, 42), and consistent with the hypothesis that cGMP plays a regulatory role in cell shape and motility during chemotaxis.

Recently, myosin II has been implicated in vesicle movement. Myosin II has been demonstrated to be associated with small cytoplasmic vesicles in *Dictyostelium* amoebae (28), and a *Dictyostelium* variant lacking myosin II (20) exhibits depressed cytoplasmic vesicle velocities and random vesicle direction in the absence of cAMP, similar to normal cells immediately after the addition of cAMP (Wessels and Soll, manuscript submitted for publication). Interestingly, cellular velocity is depressed, the rate of pseudopod extension is reduced, and cellular polarity is lost in myosin-minus variants (47), suggesting that myosin II plays a role in both vesicles and cell motility.

The results presented here demonstrate a very close relationship between cellular translocation and particle movement. Although there is no data to distinguish whether the rate and direction of cellular translocation is dependent upon the rate and direction of particle movement, or the reverse, it seems more reasonable to suggest that the former is the case. The particles that we have analyzed probably represent membrane bound vesicles (29) that may be the source of new membrane for the expanding anterior pseudopodia of rapidly translocating cells. The speed and directionality of vesicle movement in turn are probably dependent upon cytoskeletal elements that are regulated by the cAMP receptor. Testing the details of this suggested scheme will be basic to understanding chemotaxis in animal cells.

The authors are indebted to H. Vawter, F. Rogness, S. Swalwell for assistance in assembling the manuscript.

This study was supported by National Institutes of Health grants GM25832 and HD18577 to D. R. Soll, GM25813 to J. Condeelis, and by training grant funds from the National Cancer Institute (TGCA90475) and from the Hirschl Trust to A. L. Hall.

Received for publication 12 May 1989 and in revised form 28 August 1989.

References

1. Alcantara, E., and M. Monk. 1974. Signal propagation in the cellular slime mould *Dictyostelium discoideum*. *J. Gen. Microbiol.* 85:321–334.
2. Araki, N., and K. Ogawa. 1987. Regulation of intracellular lysosomal movements by the cytoskeletal system in rat alveolar macrophages. *Acta Histochem. Cytochem.* 20:659–678.
3. Bonner, J. T. 1947. Evidence for the formation of cell aggregates by chemotaxis in the development of the slime mold *Dictyostelium discoideum*. *J. Exp. Zool.* 106:1–26.
4. Condeelis, J., A. Hall, A. Bresnick, V. Warren, R. Hock, H. Bennett, and S. Ogihara. 1988. Actin polymerization and pseudopod extension during amoeboid chemotaxis. *Cell Motil. Cytoskeleton.* 10:77–90.
5. Devreotes, P. N. 1982. Chemotaxis. *In* The Development of *Dictyostelium*. W. F. Loomis, editor. Academic Press, New York. 117–168.
6. Devreotes, P. N., P. L. Derstine, and T. L. Steck. 1979. Cyclic 3',5' AMP relay in *Dictyosteluim discoideum*. I. A technique to monitor responses to controlled stimuli. *J. Cell Biol.* 80:291–299.
7. Dharmwardhane, S., V. Warren, A. Hall, and J. Condeelis. 1989. Changes in the association of actin-binding proteins with the actin cytoskeleton during chemotactic stimulation of *Dictyostelium discoideum*. *Cell Motil. Cytoskeleton.* 13:57–63.
8. Freed, J. J., and M. M. Lebowitz. 1970. The association of a class of saltatory movements with microtubules in cultured cells. *J. Cell Biol.* 45: 334–354.
9. Futrelle, R. R., J. Trant, and W. G. McKee. 1981. Cell behavior in *Dictyostelium discoideum* preaggregation response to localized cAMP pulses. *J. Cell Biol.* 92:807–821.
10. Gerisch, G., and B. Hess. 1974. Cyclic-AMP-controlled oscillations in suspended *Dictyostelium* cells: their relation to morphogenetic cell interactions. *Proc. Natl. Acad. Sci. USA.* 71:2118–2122.
11. Goldberg, D. J., D. A. Harris, B. W. Lubit, and J. H. Schwartz. 1980. Analysis of the mechanism of fast axonal transport by intracellular injection of potentially inhibitory macromolecules: evidence for a possible role for actin filaments. *Proc. Natl. Acad. Sci. USA.* 77:7448–7452.
12. Hall, A. L. The regulation of actin polymerization during chemotaxis of *Dictyostelium discoideum*. 1989 Ph.D. thesis. Albert Einstein College of Medicine, Bronx, NY. 44–56.
13. Hall, A. L., A. Schlein, and J. Condeelis. 1988. Relationship of pseudopod extension to chemotatic hormone-induced actin polymerization in ameboid cells. *J. Cell. Biochem.* 37:285–299.
14. Hegmann, T. E., J. L. Lin, and J. J. Lin. 1989. Probing the role of nonmuscle tropomyosin isoforms in intracellular granule movement by microinjection of monoclonal antibodies. *J. Cell Biol.* In press.
15. Klein, P. S., T. J. Sun, C. L. Saxe III, A. R. Kimmel, R. L. Johnson, and P. N. Devreotes. 1988. A chemoattractant receptor controls development in *Dictyostelium discoideum*. *Science (Wash. DC).* 241:1467–1472.
16. Kumagai, A., M. Pupillo, R. Gundersen, R. Miake-Lye, P. N. Devreotes, and R. A. Firtel. 1989. Regulation and function of G(alpha) protein subunits in *Dictyostelium*. *Cell.* 57:265–275.
17. Liu, G., and P. C. Newell. 1988. Evidence that cyclic GMP regulates myosin interaction with the cytoskeleton during chemotaxis of *Dictyostelium*. *J. Cell. Sci.* 90:123–129
18. Malchow, D., V. Nanjuhdiah, and G. Gerisch. 1978. pH oscillations in cell suspensions of *Dictyostelium discoideum*: their relation to cyclic-AMP signals. *J. Cell Sci.* 30:319–330.
19. Malchow, D., R. Bohme, and H. J. Rahmsdorf. 1981. Regulation of phosphorylation of myosin heavy chain during chemotactic response of *Dictyostelium* cells. *Eur. J. Biochem.* 117:213–218.
20. Manstein, D. J., M. A. Titus, A. DeLozanne, and J. Spudich. 1989. Gene replacement in *Dictyostelium*: generation of myosin null mutants. *EMBO (Eur. Mol. Biol. Organ.) J.* 8:923–932.
21. Maron, M. J. 1982. Numerical Analysis. Macmillan Publishing Co., New York. 283 pp.
22. Mato, J. M., and D. Marin-Cao. 1979. Protein and phospholipid methylation during chemotaxis in *Dictyostelium discoideum* and its relationship to calcium movements. *Proc. Natl. Acad. Sci. USA.* 76:6106–6109.
23. Mato, J., F. Krens, P. J. M. Van Haastert, and T. M. Konijn. 1977. 3',5'-cyclic AMP-dependent 3',5'-cyclic GMP accumulation in *Dictyostelium discoideum*. *Proc. Natl. Acad. Sci. USA.* 74:2348–2351.
24. McRobbie, S. J., and P. C. Newell. 1983. Changes in actin associated with the cytoskeleton following chemotactic stimulation of *Dictyostelium discoideum*. *Biochem. Biophys. Res. Commun.* 115:351–359.
25. McRobbie, S. J., and P. C. Newell. 1985. Effects of cytochalasin B on cell

movements and chemoattractant elicited actin changes in *Dictyostelium*. *Exp. Cell Res.* 160:275–286.
26. Murphy, D. B., and L. G. Tilney. 1974. The role of microtubules in the movement of pigment granules in teleost melanophores. *J. Cell Biol.* 61:757–779.
27. Newell, P. C. 1986. The role of actin polymerization in amoebae chemotaxis. *Bioessays* 5:208–211.
28. Ogihara, S., J. Carboni, and J. Condeelis. 1988. Electron microscopic localization of myosin II and ACP-120 in the cortical actin matrix of *Dictyostelium* amoebae using IgG-gold conjugates. *Dev. Genet.* 9:505–520.
29. Roos, U.-P., M. DeBrabander, and R. Nuydens. 1987. Movements of intracellular particles in undifferentiated amebae of *Dictyostelium discoideum*. *Cell Motil. Cytoskeleton.* 7:258–271.
30. Shaffer, B. M. 1957. Aspects of aggregation in the cellular slime molds. I. Orientation and chemotaxis. *Nature (Lond.).* 91:19–35.
31. Snaar-Jagalska, B. E., F. Kesbeke, and P. J. M. Van Haastert. 1988. G-proteins in the signal-transduction pathways of *Dictyostelium discoideum*. *Dev. Genet.* 9:215–226.
32. Soll, D. R. 1979. Timers in developing systems. *Science (Wash. DC).* 203:841–849.
33. Soll, D. R. 1987. Methods for manipulating and investigating developmental timing in *Dictyostelium discoideum*. *In* Methods in Cell Biology, Volume 28. J. Spudich, editor. Academic Press, New York. 413–441.
34. Soll, D. R. 1988. "DMS," a computer-assisted system for quantitating motility, the dynamics of cytoplasmic flow and pseudopod formation: its application to *Dictyostelium* chemotaxis. *Cell Motil. Cytoskeleton.* 10: 91–106.
35. Soll, D. R. 1989. Behavioral studies into the mechanism of eukaryotic chemotaxis. *J. Chem. Ecol.* In press.
36. Soll, D. R., and R. Finney. 1987. Regulation of timing during the forward program of development and the reverse program of the dedifferentiation in *Dictyostelium discoideum*. *In* Genetic Regulation of Development. W. F. Loomis, editor. Alan R. Liss, Inc., New York. 287–335.
37. Soll, D. R., E. Voss, B. Varnum-Finney, and D. Wessels. 1988. The "Dynamic Morphology System": a method for quantitating changes in shape, pseudopod formation and motion in normal and mutant amebae of *Dictyostelium discoideum*. *J. Cell. Biochem.* 37:177–192.
38. Sussman, M. 1987. Cultivation and synchronous morphogenesis of *Dictyostelium* under control experimental conditions. *In* Methods in Cell Biology, Volume 28. J. A. Spudich, editor. Academic Press, New York. 9–29.
39. Talian, J. C., J. B. Olmsted, and R. D. Goldman. 1983. A rapid procedure for preparing fluorescein-labeled specific antibodies from whole antiserum: its use in analyzing cytoskeletal architecture. *J. Cell Biol.* 97: 1277–1282.
40. Tomchick, K. J., and P. N. Devreotes. 1981. Adenosine 3',5'-monophosphate waves in *Dictyostelium discoideum*: a demonstration by isotope dilution-fluorography. *Science (Wash. DC).* 212:443–446.
41. Van Haastert, P. J. M. 1987. Differential effects of temperature on cAMP-induced excitation, adaptation, and deadaptation of adenylate and guanylate cyclase in *Dictyostelium discoideum*. *J. Cell Biol.* 105:2301–2306.
42. Van Haastert, P. M. J., R. J. W. DeWit, P. M. W. Janssens, F. Kesbeke, and J. DeBoede. 1986. G protein-mediated interconversion of cell surface cAMP receptors and their involvement in excitation and desensitization of guanyate cyclase in *Dictyostelium discoideum*. *J Biol. Chem.* 261: 6904–6911.
43. Varnum, B., and D. R. Soll. 1984. Effects of cAMP on single cell motility in *Dictyostelium*. *J. Cell Biol.* 99:1151–1155.
44. Varnum, B., K. B. Edwards, and D. R. Soll. 1985. *Dictyostelium* amebae alter motility differently in response to increasing versus decreasing temporal gradients of cAMP. *J. Cell Biol.* 101:1–5.
45. Varnum, B., K. B. Edwards, and D. R. Soll. 1986. The developmental regulation of single cell motility in *Dictyostelium discoideum*. *Dev. Biol.* 113:218–227.
46. Varnum-Finney, B., N. A. Schroeder, and D. R. Soll. 1988. Adaptation in the motility response to cAMP in *Dictyostelium discoideum*. *Cell Motil. Cytoskeleton.* 9:9–16.
47. Wessels, D., D. R. Soll, D. Knecht, W. F. Loomis, A. DeLozanne, and J. Spudich. 1988. Cell motility and chemotaxis in *Dictyostelium* amebae lacking myosin heavy chain. *Dev. Biol.* 128:164–177.
48. White, E., E. M. Tolbert, and E. R. Katz. 1983. Identification of tubulin in *Dictyostelium discoideum:* characterization of some unique properties. *J. Cell Biol.* 97:1011–1019.
49. Wick, U., D. Malchow, and G. Gerisch. 1978. Cyclic-AMP stimulated calcium influx into aggregating cells of *Dictyostelium discoideum*. *Cell Biol. Int. Rep.* 2:71–79.